Biophysical Chemistry 143 (2009) 102–105

Contents lists available at ScienceDirect

Biophysical Chemistry

journal homepage: http://www.elsevier.com/locate/biophyschem

Short communication

Dynamic force spectroscopy of the *Helicobacter pylori* BabA–Lewis b Binding

Oscar Björnham [a], Jeanna Bugaytsova [b], Thomas Borén [b], Staffan Schedin [a,*]

[a] Department of Applied Physics and Electronics, Umeå University, SE-901 87 Umeå, Sweden
[b] Department of Medical Biochemistry and Biophysics, Umeå University, SE-901 87 Umeå, Sweden

ARTICLE INFO

Article history:
Received 24 February 2009
Received in revised form 11 March 2009
Accepted 11 March 2009
Available online 19 March 2009

Keywords:
Optical tweezers
Single bond dissociation
Receptor–ligand interaction
Bond strength
Lewis b receptor

ABSTRACT

The binding strength of the *Helicobacter pylori* adhesin–receptor complex BabA-ABO/Lewis b has been analyzed by means of dynamic force spectroscopy. High-resolution measurements of rupture forces were performed *in situ* on single bacterial cells, expressing the high-affinity binding BabA adhesin, by the use of force measuring optical tweezers. The resulting force spectra revealed the mechanical properties of a single BabA–Leb bond. It was found that the bond is dominated by one single energy barrier and that it is a slip-bond. The bond length and thermal off-rate were assessed to be 0.86 ± 0.07 nm and 0.015 ± 0.006 s^{-1}, respectively.

1. Introduction

Helicobacter pylori (*H. pylori*) is a Gram-negative bacterium that causes gastritis and peptic ulceration, which can lead to gastric cancer. *H. pylori* cells are found both in the slimy mucus layer lining the gastric epithelium, and tightly attached to the epithelial cells. Some of the *H. pylori* outer membrane proteins are involved in adhesion to host tissue. The fucosylated ABO/Lewis b (Leb) blood group antigen, found in the gastric mucosa and at the gastric epithelium layer, has been well characterized as a specific receptor for the BabA adhesin. The affinity for multivalent BabA–Leb/HSA complexes, determined by Scatchard analysis during equilibrium conditions in bacterial suspensions, can be as high as 5×10^{11} M^{-1} [1].

The details underlying the molecular interaction and the mechanisms of the BabA–Leb bond are still largely unknown due to the high-affinity protein–carbohydrate binding combined with the solubility and conformational folding issues inherent with membrane proteins. This special complexity is in part due to the lack of appropriate high-resolving measurement techniques with capacity to probe single adhesin–receptor interactions. Standard methods for affinity measurements, based on equilibrium in binding, such as Scatchard analyses, hemagglutination, and various ELISA-based methods [2], are used for the assessment of interactions on bulk samples. Moreover, in high-affinity systems it is difficult to accurately establish true equilibrium in binding since the on-rate in receptor–ligand association is high, whereas the off-rate, or dissociation, is low (in experimental terms negligible). Thus, the time until true equilibrium is achieved becomes extensively long and experimentally impractical for analyses of biological systems. So, whereas several techniques for accurate measurements of affinity are available, the tools for analyses of dissociation, i.e. off-rate, have been limited. However, during recent years, dynamic force spectroscopy (DFS) has been employed for the investigation of single molecule interactions [3–6]. In this method, the minute force required to rupture a single molecular bond is measured as the bond is exposed to a gradually increasing external force. The force drastically reduces the life-time of the bond, typically on the second-to-millisecond time-scale. A spectrum of rupture forces, obtained from repeated measurements with different loading rates, provides information of important properties of the bond, e.g. the binding energy, the thermal off-rate, the bond length and whether it is a slip- or a catch-bond. Different types of instrumentations have been implemented in DFS-studies. These instrumentations include atomic force microscopy [7–10], biomembrane force probes [11–13] and force measuring optical tweezers [14–16].

In the present study, we used a force measuring optical tweezers (FMOT) for precise, *in situ*, measurements of the rupture forces between a single BabA adhesin on the surface of single *H. pylori* bacterial cells and its receptor. We present novel results with detailed analyses of the *H. pylori* BabA–Leb binding strength that classifies and defines the bond.

2. Materials and methods

2.1. Force measuring optical tweezers

The optical tweezers system is based on an inverted Olympus IX71 microscope with a high numerical aperture oil-immersion objective lens (Olympus UPlanF1 100×). The trapping laser is a continuous-wave 1064 nm Nd:YVO_4 laser (Spectra-Physics, Millennia IR10). A HeNe-laser serves as a probe laser (1137, Uniphase, Manteca), and is directed into the optical path of the trapping beam to detect the

* Corresponding author. Tel.: +46 90 786 7487; fax: +46 90 786 6469.
E-mail addresses: oscar.bjornham@tfe.umu.se (O. Björnham), jeanna.bugaytsova@medchem.umu.se (J. Bugaytsova), thomas.boren@medchem.umu.se (T. Borén), staffan.schedin@tfe.umu.se (S. Schedin).

0301-4622/$ – see front matter © 2009 Elsevier B.V. All rights reserved.
doi:10.1016/j.bpc.2009.03.007

position of a trapped bead. If the trapped bead is displaced a short distance due to an external force it redirects the probe laser beam which is monitored in the far-field with a position-sensitive detector (SiTek Electro Optics, Partille, Sweden). A two-step calibration method is implemented to quantify the exerted force (in pN) on the trapped bead. First, the response of the position-sensitive detector is determined, i.e. a calibration factor that converts the voltage of the detector signal to a position (in nm) of the trapped bead. This is done by means of a sequence of controlled trap displacements. Second, the stiffness of the trap is determined from the power spectrum of the thermal fluctuation of the trapped bead. The fluctuation of the bead is described theoretically by the Brownian motion from the surrounding medium under the constraint set by the trap. The trap stiffness is thereby assessed by fitting the theoretical curve, derived from the Langevin equation [17], to the measured data. A detailed description of the system is given by Fällman et al. and Andersson et al. [18,19].

2.2. Bacterial strains and Lewis b receptor

The *H. pylori* strains used in this study are 17875/Leb and 17875babA1::kan babA2::cam (abbreviated 17875*babA1A2*). The 17875/Leb strain used for BabA-dependent measurements is a spontaneous mutant of strain CCUG 17875 and binds Leb [20]. As a relevant control for accurate specificity of the BabA–Leb binding, the 17875*babA1A2*-mutant, devoid of the BabA adhesin, was used to assess non-specific binding. Bacteria were grown on *Brucella* agar supplemented with 10% bovine blood and 1% IsoVitalex (Svenska LABFAB, Ljusne Sweden), for 30–40 h at 37 °C in 10% CO_2 and 5% O_2 before harvest in phosphate-buffered saline (PBS) containing 0.05% Tween 20 and 1% bovine serum albumin (BSA) (Sigma-Aldrich, Stockholm, Sweden).

The glycoconjugate used is Leb/HSA, i.e. human serum albumin to which the adhesin Lewis b glycans were chemically attached (IsoSep AB, Tullinge, Sweden).

2.3. Biological model system and measurement procedure

The biological model system was compounded by the following components: a cover glass with large poly-L-lysine-coated beads (~9 μm) attached to its surface (Sigma-Aldrich, Stockholm, Sweden/Interfacial Dynamics Corporation, Portland, Oregon), the bacterial cells diluted to a low concentration (~10^5 μl^{-1}) and small Leb/HSA coated beads (~3.2 μm), suspended in PBS [21]. The sample of ~25 μl was confined in between two glass coverslips, separated by ~1 mm, which constituted a closed chamber. This chamber was placed in a custom made aluminium slide holder under the microscope in the optical tweezers system. A piezo-electrical stage (Physik Instrumente, Karlsruhe, Germany) was used for precise translation of the chamber with the sample. The experiments were performed at ~25 °C and at pH 7.4, which corresponds to the close neutral pH conditions in the epithelial lining, with a buffer of PBS (1×) with 1% BSA. The presence of the blocking agent BSA efficiently reduces non-specific interactions.

In the force measurement procedure, a free-floating bacterium was trapped by the tweezers and brought into contact with a fixed large bead, so as to form strong electrostatic bindings between the positively charged poly-L-lysine and negatively charged bacterium cell membrane. To minimize the risk of damage to the trapped bacterium, the power of the trapping laser was reduced by a factor of 10 when a bacterium was trapped which resulted in an exposure of the sample of ~10 mW laser power. Next, a small Leb coated bead was trapped, with normal power of the trapping laser, and the two-step calibration procedure was performed. A single BabA–Leb binding was then formed by bringing the bacterial cell and the trapped bead into initial contact. To minimize the formation of multiple bindings, the contact time was short (~0.1 s). Next, the large bead, with the bacterium, was retracted with a constant velocity and the force in the system was recorded until the binding ruptured, see Fig. 1A. This procedure gives rise to a linearly increased force on the bond. A detailed description of the measurement procedure is given by Björnham et al. [21].

2.4. Bond kinetics

The assessment of the BabA–Leb bond properties is based on the Bell–Evans theory of bond kinetics [22,23]. The thermal off-rate for a binding, $k^{\mathrm{th}}_{\mathrm{off}}$, can be described by the relation

$$k^{\mathrm{th}}_{\mathrm{off}} = \upsilon e^{-\frac{E}{k_B T}}, \tag{1}$$

where υ is the attempt rate, E is the height of the energy barrier, k_B is the Boltzmann's constant and T is the absolute temperature. In the presence of an external force, f, the off-rate for a binding, k_{off}, is increases exponentially as

$$k_{\mathrm{off}} = k^{\mathrm{th}}_{\mathrm{off}} e^{\frac{fx_b}{k_B T}}, \tag{2}$$

where x_b is the distance to the activation barrier, here referred to as the *bond length*. A schematic energy landscape as well as the effective linear tilting thereof, which originates from an external force, is given in Fig. 1B. An external force that increases with a constant rate, r, induces a maximum in the rupture force distribution, f^*, defined as the *bond strength* in this work, which is given by

$$f^* = \frac{k_B T}{x_b} \ln\left(\frac{r x_b}{k^{\mathrm{th}}_{\mathrm{off}} k_B T}\right). \tag{3}$$

Eq. (3) predicts that the bond strength scales logarithmically with the loading rate. This relationship is used to explore the properties of

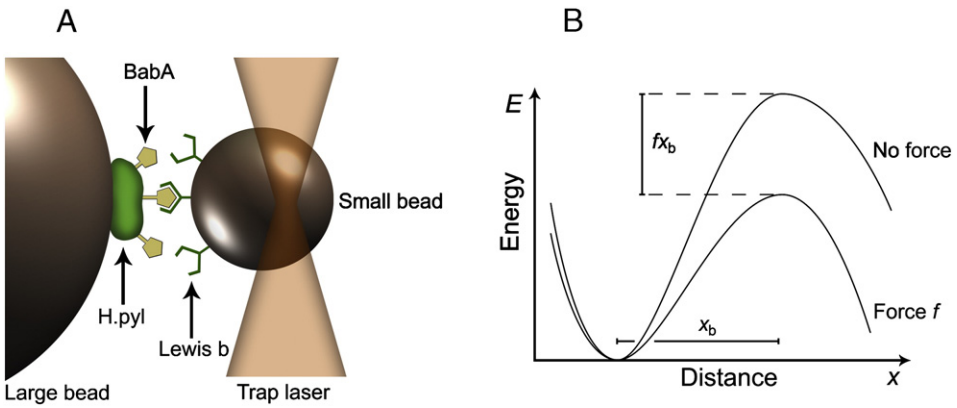

Fig. 1. Panel A, a conceptual illustration of the force measuring procedure with the optical tweezers system. Panel B, a schematic drawing of the energy landscape. An external force, f, tilts the landscape linearly which increases the probability for rupture.

the bond. The bond strength at different loading rates reveals both the bond length and the thermal off-rate.

The shape of the theoretical distribution of forces is not symmetric around the bond strength which implies that the mean value of the distribution of rupture forces diverges from the bond strength. For low forces, the error of the thermal off-rate when the mean value of the rupture forces is used, approaches an astonishing 70% [24]. For an accurate assessment of the bond parameters in this work, we therefore use the exact solution for the rupture probability density function, $\rho(f)$, [25]

$$\rho(f) = \frac{k_{\mathrm{off}}^{\mathrm{th}}}{r} e^{\frac{fx_b}{k_B T}} e^{-k_{\mathrm{off}}^{\mathrm{th}} \frac{k_B T}{r x_b}\left(e^{\frac{fx_b}{k_B T}} - 1\right)}. \quad (4)$$

2.5. Processing of experimental data

The rupture force data result in a distribution, assembled by means of a kernel density estimator, which is subjected to a fitting procedure where the maximum of the fitting function corresponds to the bond strength, f^*. Even though the measured rupture probability density is not expected to be symmetric around the maximum value, a Gaussian fit is often applied to measured distributions in order to find the peak [12,26–30]. However, the theoretical distribution function, Eq. (4), represents the expected shape of the measured rupture force distribution and returns far more accurate bond strengths than a Gaussian does. For this reason, Eq. (4) was used for the assessment of the bond strength in this work.

The uncertainties of the fitting parameters to experimental data gave rise to errors in the final parameters such as bond lengths and thermal off-rates. The 95%-confidential intervals of these parameters, presented below, were calculated by monitoring the propagation of the fitting uncertainties throughout the complete analyses.

3. Results and discussion

An example of a force-curve for the Leb–BabA interaction is presented in Fig. 2A. The FMOT-system measures forces with high resolution, the noise level amounts approximately to ~2 pN peak-to-peak. Rupture forces were extracted from a large number of measurements on single cells at four different loading rates (2 700, 480, 68 and 6.8 pN/s). These loading rates are the *effective loading rates* for the binding when the influence from the stiffness of the bacterium body [21] has been compensated for. The results presented below are based on 855 single measurements on strain 17875/Leb, and 722 negative control measurements on the 17875*babA1A2*-mutant. The data provide a spectrum with four bond strengths which enables precise analyses of the bond length and the thermal off-rate of the BabA–HSA/Leb binding pair.

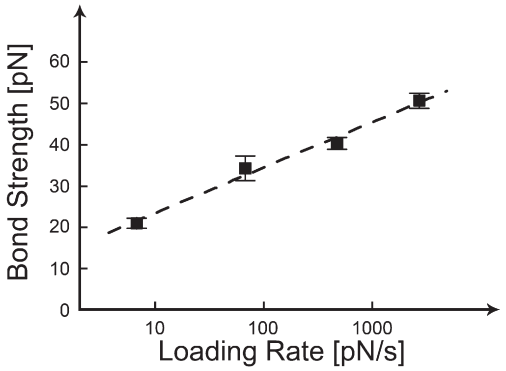

Fig. 3. The dynamic force spectra for the BabA–Leb binding where the error bars represent 95% confidential intervals. The best linear fit, with respect to the mean square error, is illustrated by a dashed line.

Fig. 2B displays continuous rupture probability density estimator for the 17875/Leb (solid gray area) and for the 17875*babA1A2*-mutant (dashed gray area) for the loading rate of 2 700 pN/s. A fit, based on Eq. (4), is applied to the force distribution (dashed line) in order to assess the bond strength, here 50.6 pN. The rupture force distribution is well reproduced by the fit although the measured data exhibit a relatively extended tail at high forces. This tail is attributed to occasional occurrences of multiple bindings as virtually no unspecific interactions were observed in this interval. Similar continuous density estimations and fits, to assess the bond strengths, were carried out for the other three loading rates. The resulting bond strengths for different loading rates are presented in Fig. 3 together with the best linear fit with respect to the mean square error.

For assessment of the binding properties, we analyze the relation between the bond strengths and the loading rate. Fig. 3 reveals that the bond strengths increase linearly with the logarithm of the loading rate, which is in accordance with the analytical expression Eq. (3). The bond length was obtained from the slope of the linear fit and is $x_b = 0.86 \pm 0.07$ nm. In addition, the thermal off-rate is also retrieved from the intersection of the extrapolated linear fit with the horizontal axis and is $k_{\mathrm{off}}^{\mathrm{th}} = 0.015 \pm 0.006\ \mathrm{s}^{-1}$. The binding energy is obtained by inserting the thermal off-rate into Eq. (1) and amounts to 26.5 $k_B T$. Here we have assumed an attempt rate of $5 \times 10^9\ \mathrm{s}^{-1}$ which is in the middle of the interval of $10^9 - 10^{10}\ \mathrm{s}^{-1}$ reported by Evans et al. and Merkel et al. [12,27].

The thermal off-rate for the Leb–BabA binding is similar to other binding systems [3,28,31] but also significantly higher than the well examined streptavidin–biotin complex [5,32]. The fact that the thermal off-rate presented here is not as low as might be expected

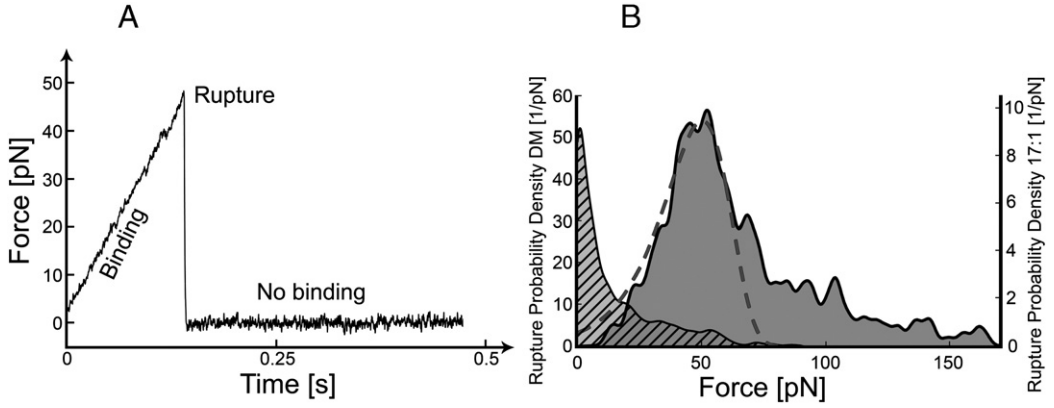

Fig. 2. Panel A shows data from a typical force measurement. The force increases linearly until the bond ruptures whereafter the force drops immediately to zero. Panel B shows measured rupture data for the effective loading rate 2700 pN/s. The continuous density estimators refer to the 17875/Leb (solid grey) and to the 17875*babA1A2*-mutant (dashed grey), respectively. The two density estimators have individual vertical axes. A fit, based on Eq. (4), is applied to the distribution for the 17875/Leb which provides the bond strength, 50.6 pN. The area under the curves corresponds to the number of measurements that sums up the density estimators for the 17875*babA1A2*-mutant and the 17875/Leb, respectively.

Table 1
Comparison between different bindings in a similar range of loading rates.

Binding	x_b [nm]	k_{off}^{th} [$\times 10^{-3}$ s^{-1}]	Reference
Digoxigenin/anti-digoxigenin	1.15	15	Neuert et al. [3]
Streptavidin/biotin	0.49	0.0167	Yuan et al. [5]
Lysozyme/FV-antibody	1.0	1.0	Berquand et al. [34]
PapG/galabiose	0.50	2.6	Bjornham et al. [14]
Protein A/immunoglobulinG	1.12	14.3	Salomo et al. [31]
LexA/recA	0.54	45	Kuhner et al. [36]
BabA–Lewis b	0.86	15	Presented here

from the very high affinity, suggests that *H. pylori* bind with a high degree of multivalence. The bond length for the Leb–BabA bond presented here is in the same interval as that for other receptor–ligand systems [3,5,12,33–36]. Examples of data of off-rates and bond lengths obtained by dynamic force spectroscopy in other specific protein–ligand complexes are given in Table 1.

The fact that the rupture probability density estimators exhibit local maxima implies that the BabA–Leb binding is a slip-bond within the range of the forces applied here, i.e. the off-rate increases with the external force. Further on, the linearity of the bond strength with respect to the logarithm of the loading rate suggests that the BabA–Leb bond is well described by Bell's kinetic theory with a single transition state in this interval of loading rates.

What are the *in vivo* implications of the binding properties obtained in this work? It is reasonable to assume that the forces due to shear flow are higher further out from the mucus layer which implies that the off-rate will increase when the bacterium approach the corpus since it is a slip-bond. This property is advantageous in this context since it suggests a functional regulation mechanism of *H. pylori* adherence *in vivo* that allows a bacterium attached to a shedded cell in the corpus to detach and swim back and reattach to the epithelial cells.

Acknowledgement

This work was supported by grants from the Magn. Bergvalls Foundation and the Swedish Research Council/VRNT (SS); Swedish Research Council/VRM (TB), Cancerfonden (TB), Umeå University Biotechnology Fund (TB), the J.C. Kempe and Seth M. Kempe Memorial Foundation (TB), SSF programs, "Glycoconjugates in Biological Systems" (T.B.), and the EU FP6 EuroPathoGenomics Network of Excellence (TB).

We thank U.J. Nilsson for providing Leb coated beads and E. Fällman, M. Andersson as well as R. Sjöström for technical assistance and good discussions.

References

[1] M. Aspholm, F.O. Olfat, J. Norden, B. Sonden, C. Lundberg, R. Sjostrom, S. Altraja, S. Odenbreit, R. Haas, T. Wadstrom, L. Engstrand, C. Semino-Mora, H. Liu, A. Dubois, S. Teneberg, A. Arnqvist, T. Boren, SabA is the H. pylori hemagglutinin and is polymorphic in binding to sialylated glycans e110, Plos Pathogens 2 (2006) 989–1001.
[2] M. Aspholm, A. Kalia, S. Ruhl, S. Schedin, A. Arnqvist, S. Linden, R. Sjostrom, M. Gerhard, C. Semino-Mora, A. Dubois, M. Unemo, D. Danielsson, S. Teneberg, W.K. Lee, D.E. Berg, T. Boren, *Helicobacter pylori* Adhesion to Carbohydrates, Elsevier Academic Press Inc, San Diego, USA, 2006.
[3] G. Neuert, C. Albrecht, E. Pamir, H.E. Gaub, Dynamic force spectroscopy of the digoxigenin–antibody complex, FEBS Letters 580 (2006) 505–509.
[4] E. Evans, A. Leung, V. Heinrich, C. Zhu, Mechanical switching and coupling between two dissociation pathways in a P-selectin adhesion bond, Proceedings of the National Academy of Sciences of the United States of America 101 (2004) 11281–11286.
[5] C.B. Yuan, A. Chen, P. Kolb, V.T. Moy, Energy landscape of streptavidin–biotin complexes measured by atomic force microscopy, Biochemistry 39 (2000) 10219–10223.
[6] X.H. Zhang, E. Wojcikiewicz, V.T. Moy, Force spectroscopy of the leukocyte function-associated antigen-1/intercellular adhesion molecule-1 interaction, Biophysical Journal 83 (2002) 2270–2279.
[7] C.K. Lee, Y.M. Wang, L.S. Huang, S.M. Lin, Atomic force microscopy: determination of unbinding force, off rate and energy barrier for protein–ligand interaction, Micron 38 (2007) 446–461.
[8] M. Odorico, J.M. Teulon, O. Berthoumieu, S.W.W. Chen, P. Parot, J.L. Pellequer, An integrated methodology for data processing in dynamic force spectroscopy of ligand-receptor binding, Ultramicroscopy 107 (2007) 887–894.
[9] X.H. Zhang, D.F. Bogorin, V.T. Moy, Molecular basis of the dynamic strength of the sialyl Lewis X-selectin interaction, Chemphyschem 5 (2004) 175–182.
[10] A. Fuhrmann, D. Anselmetti, R. Ros, S. Getfert, P. Reimann, Refined procedure of evaluating experimental single-molecule force spectroscopy data, Physical Review E 77 (2008).
[11] E. Perret, A. Leung, H. Feracci, E. Evans, Trans-bonded pairs of E-cadherin exhibit a remarkable hierarchy of mechanical strengths, Proceedings of the National Academy of Sciences of the United States of America 101 (2004) 16472–16477.
[12] R. Merkel, P. Nassoy, A. Leung, K. Ritchie, E. Evans, Energy landscapes of receptor–ligand bonds explored with dynamic force spectroscopy, Nature 397 (1999) 50–53.
[13] W. Chen, E.A. Evans, R.P. McEver, C. Zhu, Monitoring receptor–ligand interactions between surfaces by thermal fluctuations, Biophysical Journal 94 (2008) 694–701.
[14] O. Bjornham, H. Nilsson, M. Andersson, S. Schedin, Physical properties of the specific PapG-galabiose binding in E-coli P pili-mediated adhesion, European Biophysics Journal with Biophysics Letters 38 (2009) 245–254.
[15] M. Arya, A.B. Kolomeisky, G.M. Romo, M.A. Cruz, J.A. Lopez, B. Anvari, Dynamic force spectroscopy of glycoprotein Ib-IX and von Willebrand factor, Biophysical Journal 88 (2005) 4391–4401.
[16] P. Bianco, A. Nagy, A. Kengyel, D. Szatmari, Z. Martonfalvi, T. Huber, M.S.Z. Kellermayer, Interaction forces between F-actin and titin PEVK domain measured with optical tweezers, Biophysical Journal 93 (2007) 2102–2109.
[17] F. Gittes, C.F. Schmidt, Thermal noise limitations on micromechanical experiments, European Biophysics Journal 27 (1998) 75–81.
[18] E. Fällman, S. Schedin, J. Jass, M. Andersson, B.E. Uhlin, O. Axner, Optical tweezers based force measurement system for quantitating binding interactions: system design and application for the study of bacterial adhesion, Biosensors and Bioelectronics 19 (2004) 1429–1437.
[19] M. Andersson, E. Fällman, B.E. Uhlin, O. Axner, Dynamic force spectroscopy of the unfolding of P pili, Biophysical Journal 91 (2006) 2717–2725.
[20] J. Mahdavi, B. Sonden, M. Hurtig, F.O. Olfat, L. Forsberg, N. Roche, J. Angstrom, T. Larsson, S. Teneberg, K.A. Karlsson, S. Altraia, T. Wadstrom, D. Kersulyte, D.E. Berg, A. Dubois, C. Petersson, K.E. Magnusson, T. Norberg, F. Lindh, B.B. Lundskog, A. Arnqvist, L. Hammarstrom, T. Boren, *Helicobacter pylori* SabA adhesin in persistent infection and chronic inflammation, Science 297 (2002) 573–578.
[21] O. Björnham, E. Fällman, O. Axner, J. Ohlsson, U. Nilsson, T. Borén, S. Schedin, Measurements of the binding force between the *Helicobacter pylori* adhesin BabA and the Lewis b blood group antigen using optical tweezers, Journal of Biomedical Optics 10 (2005) 044024.
[22] M.G. Bell, Models for the specific adhesion of cells to cells, Science 200 (1978) 618–627.
[23] E. Evans, K. Ritchie, Dynamic strength of molecular adhesion bonds, Biophysical Journal 72 (1997) 1541–1555.
[24] P.M. Williams, Analytical descriptions of dynamic force spectroscopy: behaviour of multiple connections, Analytica Chimica Acta 479 (2003) 107–115.
[25] J. Husson, F. Pincet, Analyzing single-bond experiments: influence of the shape of the energy landscape and universal law between the width, depth, and force spectrum of the bond, Physical Review E 77 (2008).
[26] V. Dupres, F.D. Menozzi, C. Locht, B.H. Clare, N.L. Abbott, S. Cuenot, C. Bompard, D. Raze, Y.F. Dufrene, Nanoscale mapping and functional analysis of individual adhesins on living bacteria, Nature Methods 2 (2005) 515–520.
[27] E. Evans, Energy landscapes of biomolecular adhesion and receptor anchoring at interfaces explored with dynamic force spectroscopy, Faraday Discussions 111 (1998) 1–16.
[28] F. Schwesinger, R. Ros, T. Strunz, D. Anselmetti, H.J. Guntherodt, A. Honegger, L. Jermutus, L. Tiefenauer, A. Pluckthun, Unbinding forces of single antibody–antigen complexes correlate with their thermal dissociation rates, Proceedings of the National Academy of Sciences of the United States of America 97 (2000) 9972–9977.
[29] S.M. Lin, Y.M. Wang, L.S. Huang, C.W. Lin, S.M. Hsu, C.K. Lee, Dynamic response of glucagon/anti-glucagon pairs to pulling velocity and pH studied by atomic force microscopy, Biosens. Bioelectron. 22 (2007) 1013–1019.
[30] E. Evans, Looking inside molecular bonds at biological interfaces with dynamic force spectroscopy, Biophysical Chemistry 82 (1999) 83–97.
[31] M. Salomo, U.F. Keyser, M. Struhalla, F. Kremer, Optical tweezers to study single Protein A/Immunoglobulin G interactions at varying conditions, European Biophysics Journal with Biophysics Letters 37 (2008) 927–934.
[32] L.A. Klumb, V. Chu, P.S. Stayton, Energetic roles of hydrogen bonds at the ureido oxygen binding pocket in the streptavidin–biotin complex, Biochemistry 37 (1998) 7657–7663.
[33] E. Evans, Probing the relation between force – lifetime – and chemistry in single molecular bonds, Annual Review of Biophysics and Biomolecular Structure 30 (2001) 105–128.
[34] A. Berquand, N. Xia, D.G. Castner, B.H. Clare, N.L. Abbott, V. Dupres, Y. Adriaensen, Y.F. Dufrene, Antigen binding forces of single antilysozyme Fv fragments explored by atomic force microscopy, Langmuir 21 (2005) 5517–5523.
[35] O. Takeuchi, T. Miyakoshi, A. Taninaka, K. Tanaka, D. Cho, M. Fujita, S. Yasuda, S.P. Jarvis, H. Shigekawa, Dynamic-force spectroscopy measurement with precise force control using atomic-force microscopy probe, Journal of Applied Physics 100 (2006).
[36] F. Kuhner, L.T. Costa, P.M. Bisch, S. Thalhammer, W.M. Heckl, H.E. Gaub, LexA-DNA bond strength by single molecule force spectroscopy, Biophys. J. 87 (2004) 2683–2690.